INTERFACIAL INTERACTIONS AND THE HETEROGENEOUS ONE-ELECTRON REDUCTION OF METHYL VIOLOGEN

Michael HEYROVSKÝ and Ladislav NOVOTNÝ

The J. Heyrovský Institute of Physical Chemistry and Electrochemistry, Czechoslovak Academy of Sciences, 118 40 Prague 1

Received July 22nd, 1986

The one-electron reversible electroreduction of methyl viologen to its radical cation in aqueous solutions on mercury electrodes proceeds, according to potential, concentration and time of electrolysis, in various ways. Methyl viologen is adsorbed in flat orientation at the electrode surface; it undergoes a surface redox process in π-interaction with the metal in a potential range positive by about 0·2 V of the beginning of the electroreduction. The actual reduction starts by electron transfer followed by adsorption of the radical cation and, at higher concentrations and in a narrow potential range, by crystallization at the electrode surface of a salt of the radical cation. In solution near the electrode the radical cation dimerizes and the dimer also adsorbs at the electrode. In the region of the standard redox potential and more negative the reduction proceeds by electron transfer from the electrode covered by a layer of the radical cation or of its dimer.

The 1,1'-dimethyl-4,4'-bipyridylium ion, or the methyl viologen[1] dication, MV^{2+}, is a species frequently used in electron transfer processes in solutions (see, *e.g.*[2-4]), convenient for the ease with which it accepts an electron forming the blue radical cation $MV^{+\cdot}$ and for the relatively negative redox potential[5] characterizing this reversible reaction.

The radical cation $MV^{+\cdot}$ has a tendency to dimerize[6-8] which is particularly pronounced in water and which has to be taken into account when considering redox equilibria.

From the amount of experimental data published in literature (*e.g.*[9-14]) it appears that, due to the ready adsorption of both the dication and the radical cation on various surfaces, the heterogeneous electron transfer reaction of MV^{2+} is a considerably more complex process than the homogeneous one. Because of wide use of methyl viologen in heterogeneous and microheterogeneous systems its heterogeneous reactivity is of special interest; the reproducibly renewed mercury electrode as a simplest heterogeneous system provides ideal means for its study. In our previous paper[15] we dealt with interfacial interactions between mercury and the parent molecule of MV^{2+}, the 4,4'-bipyridyl. The present paper brings results of combined polarographic and electrocapillary measurements carried out with the aim to understand the processes which enter into the heterogeneous one-electron reduction of the MV^{2+} ion at mercury electrode in aqueous solutions.

EXPERIMENTAL

Electrocapillary measurements were carried out with a spindle-type dropping mercury electrode by the method of controlled convection[16,17]. The capillaries, the apparatus, the chemicals and the procedure with the solutions were the same as described previously[15]. In addition, for recording polarographic and voltammetric curves the GWP 675 polarograph (ZWG, Academy of Sciences of G.D.R., Berlin) with an Endim 620.02 XY recorder was used. Methyl viologen was dichloride, a Fluka product. All values of potentials given in the paper are referred to the saturated calomel electrode (SCE).

RESULTS AND DISCUSSION

Thanks to the work of several authors[18–23] the main features of the electroreduction of MV^{2+} are known. The MV^{2+} dication accepts the first electron in a reversible, pH-independent step in which the blue radical cation $MV^{+\cdot}$ is formed; the corresponding polarographic half-wave potential $E_{1/2} = -0{\cdot}69$ V (*vs* SCE) is in agreement with the potentiometrically measured redox potential[5,24]. The complexity of the electrode process becomes clearly apparent when the polarographic curves are compared over a wider concentration range starting from low concentrations.

A precise study of the dependence of the d.c. polarographic curve on the pressure of mercury at various concentrations of MV^{2+} shows that the faradayic as well as non-faradayic currents depend on adsorption and that the corresponding adsorption equilibria are not always attained during the drop-time. The limiting current of reduction of MV^{2+} to $MV^{+\cdot}$, *e.g.*, is purely diffusion controlled only at concentrations $7 \cdot 10^{-5}$ mol l^{-1} and higher – this dependence has been found for the entire cathodic current measured from zero, *i.e.*, including the component due to charging of the electrode. From the results of previous measurements[10,25] and from what is shown below it follows that at about the concentration $7 \cdot 10^{-5}$ mol l^{-1} the dropping electrode is being completely covered during its growth by the reduction products, the radical cation $MV^{+\cdot}$ or its dimer, MV_2^{2+}, which have displaced the cations of the supporting electrolyte from the closest contact with the electrode surface and thus become the sole bearers of the charging current at the negatively charged electrode. In this way the sum of both currents, the faradayic and the nonfaradayic, is controlled by diffusion of MV^{2+} to the electrode and of the reduction products from the electrode.

Fig. 1 shows changes of the mean current of the d.c. polarographic curve in the potential region of the first reduction step when the concentration of MV^{2+} in solution is varied between $1 \cdot 10^{-5}$ and $5 \cdot 10^{-4}$ mol l^{-1}. Three different waves can be distinguished on the curves: from the lowest MV^{2+} concentrations increases the first, drawn-out prewave with $E_{1/2}$ around $-0{\cdot}50$ V and reaches its limiting height at about $5 \cdot 10^{-5}$ mol l^{-1}; at higher concentrations the main wave starts appearing on top of the prewave and continues growing proportionally with concentration – by its $E_{1/2}$ which does not change with concentration it can be identified as per-

taining to the electron transfer proper, $MV^{2+} + e \rightleftharpoons MV^{+\cdot}$; an additional wave appears at concentration about $2 \cdot 10^{-4}$ mol l^{-1} between the first prewave and the main wave and when MV^{2+} concentration is further increased it shifts, maintaining constant height, towards positive potentials. For a correct interpretation of the three different processes connected with the one-electron heterogeneous reduction of MV^{2+} it is important to know the parameters of the adsorption equilibrium of MV^{2+} and the tendency to adsorption of its reduction products over the corresponding potential range, such as are provided in electrocapillary measurements by the method of controlled convection[16,17].

Electrocapillary Measurements

The electrocapillary curves of MV solutions for concentrations between $5 \cdot 10^{-7}$ and $2 \cdot 10^{-4}$ mol l^{-1} are shown in Fig. 2. They indicate strong adsorption on mercury of MV^{2+} as well as of its reduction products. The inflection at $-0{\cdot}7$ V marks the first reduction step. The dashed line denotes the potential range of the electrolytic process where adsorption is combined with electron transfer and transport processes. The scatter of points at curve 7 characterizes a particular region where no reprodu-

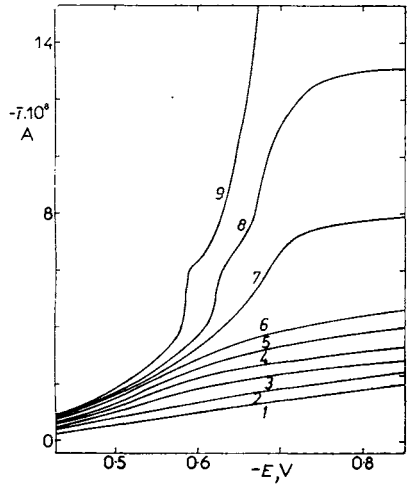

FIG. 1

D.c. polarographic curves corresponding to the first reduction step of MV^{2+}. 0·1M $NaClO_4$, concentration of $MVCl_2$: *1* 0; *2* 1; *3* 2; *4* 3; *5* 4; *6* 5; *7* 10; *8* 20; *9* 50 . 10^{-5} mol l^{-1}

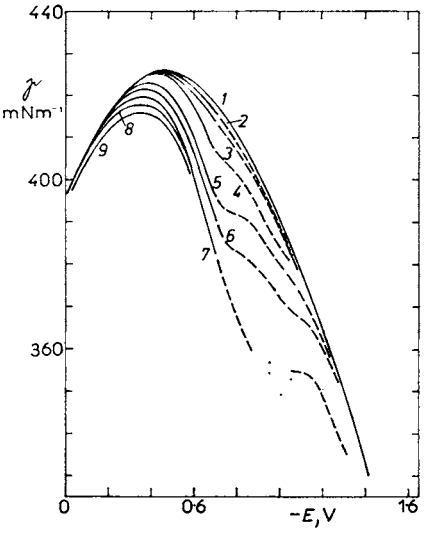

FIG. 2

Electrocapillary curves in 0·1M $NaClO_4$ in presence of $MVCl_2$ in concentration: *1* 0; *2* 0·5; *3* 1; *4* 2; *5* 10; *6* 20; *7* 50; *8* 100; *9* 200 . 10^{-6} mol l^{-1}

cible drop-time can be obtained. The surface tension values for the potential range positive of the first reduction wave are given in Table I.

From the data of the electrocapillary curves a set of γ–log c curves were plotted for constant potential values between $-0{\cdot}1$ and $-0{\cdot}65$ V in 50 mV intervals and from those by graphical differentiation according to the Gibbs–Lippmann equation for the surface excess Γ, $\Gamma = -(1/2{\cdot}303RT)(\partial\gamma/\partial \log c)$, the Γ–E curves for various concentrations were obtained (Fig. 3). Comparison of Figs 2 and 3 shows that MV^{2+} is adsorbed already on positively charged electrode. The conjugated system of the two aromatic nuclei of MV^{2+} is known to enter readily into charge transfer interaction with electron-rich species in homogeneous media[4] and it can be expected that an analogous interaction occurs in planar adsorption at a pure metallic surface, like in the case of the bipyridylium ion[15]. The π-interaction between the aromatic system and the electrons in the metal is hence stronger than the electrostatic repulsion of the dication from the positive surface, weakend, presumably, by association of MV^{2+} with anions in the interface[26]. However, unlike in the case of the structurally closely related 4,4′-bipyridylium ion[15], the MV^{2+} adsorption has its limit at positive potentials. This is probably due to the hydrophobic character of MV^{2+} compared with the more hydrophilic bipyridylium ion which in an electrical repelling field can turn with one end towards the solution and eventually, after splitting off the proton from the positively charged nitrogen atom facing the electrode, go over from non-localized to localized interaction with mercury. The symmetrical hydrophobic MV^{2+}

TABLE I

Equilibrium interfacial tension of Hg in aqueous solution of $MVCl_2$ in 0·1M $NaClO_4$ (mN m^{-1} with precision of $\pm 0{\cdot}2$ mN m^{-1})

$-E$ V *vs* SCE	Concentration of $MVCl_2$ mol l^{-1}								
	0	$5 . 10^{-7}$	$1 . 10^{-6}$	$2 . 10^{-6}$	$1 . 10^{-5}$	$2 . 10^{-5}$	$5 . 10^{-5}$	$1 . 10^{-4}$	$2 . 10^{-4}$
0·000	396·0	396·0	396·0	396·0	396·0	396·0	396·0	—	—
0·050	401·5	401·5	401·5	401·5	401·5	401·5	401·5	400·9	399·5
0·100	407·1	407·1	407·1	407·1	407·1	407·1	407·1	406·0	404·3
0·150	411·6	411·6	411·6	411·6	411·6	411·6	411·5	410·1	408·2
0·200	415·7	415·7	415·7	415·7	415·7	415·6	415·0	413·5	413·2
0·250	419·2	419·2	419·2	419·2	419·2	418·5	417·4	416·0	414·1
0·300	421·8	421·8	421·8	421·8	421·5	420·4	419·0	417·4	415·4
0·350	423·8	423·8	423·8	423·8	422·5	421·3	419·6	417·6	415·6
0·400	425·1	425·0	424·9	424·6	422·6	421·3	419·2	417·2	415·1
0·450	425·8	425·5	425·1	424·5	421·6	419·9	417·6	415·6	413·5
0·500	425·5	425·0	424·4	423·4	419·5	417·3	414·4	412·5	410·8
0·550	424·8	423·7	422·7	421·1	415·6	412·5	409·1	407·3	406·0

dication either approaches the electrode in parallel with the surface or, at positive potentials where the electrostatic repulsion prevails, does not enter the interface at all. The methyl group bound to nitrogen prevents the localized interaction of the *N* atom of MV^{2+} with mercury. On the other hand, for both ions is similar the increase of adsorption with increasing negative potential of the electrode; this tendency is more strongly pronounced in MV^{2+}. Up to the concentration $2 \cdot 10^{-5}$ mol l^{-1} of MV^{2+} the curves of Γ *vs* E are monotonous. At higher concentrations the curves go through an inflection at about $-0{\cdot}35$ V, *i.e.*, at a potential corresponding to the maximum of electrocapillary curves in the given solutions, and at more negative potentials they cross over the curves of lower concentrations. This nonmonotonous course of the Γ–E curves at higher concentrations is presumably due to special associations of MV^{2+} with anions in the less negative and of $MV^{+\cdot}$ in the more negative regions of potentials. In solutions of $MVCl_2$ (ref[27]), and in particular in the interface[26], the dication MV^{2+} associates with Cl^- anions; the asymmetrical complex $MV^{2+}Cl^-$ or the pairs $MV^{2+}X^-$, where X^- stands for other anions in the solution, get adsorbed near the potential of zero charge in a position inclined to the electrode surface – hence the increase of surface excess. When in $NaClO_4$ as supporting electrolyte at higher concentrations of MV^{2+} the $MV^{+\cdot}$ radical cation is generated by the faradayic process, a crystallization of sparingly soluble $MV^{+\cdot}ClO_4^-$ takes place at the electrode surface, as is discussed below. This results in a particular space requirement by the new phase, larger than for simple adsorption of the radical cation, which explains the crossing of the Γ–E curves.

From the Γ–E curves the dependence of surface excess Γ on the bulk concentration c, or the adsorption isotherms, can be obtained for various values of constant

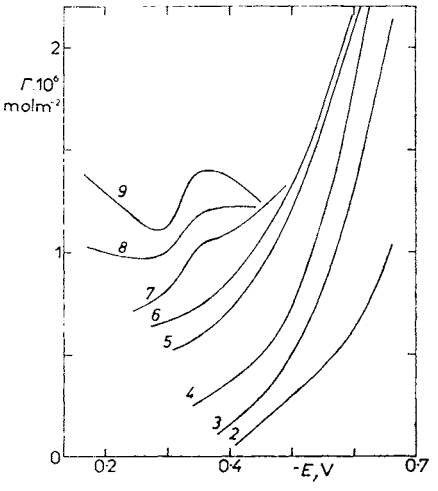

FIG. 3

Dependence of the surface excess Γ on potential obtained from the curves in Fig. 2 (corresponding curves numbering)

potential, E, and are shown in Fig. 4. The isotherms indicate that already at the bulk concentration of $2 \cdot 10^{-5}$ mol l^{-1} the electrode surface is nearly completely covered by adsorbed MV^{2+}. It is worth noticing that at positive potentials where the adsorption is weaker the ascending part of the isotherm acquires an S-shape. Similar result was observed also with other adsorptive substances[16,28]. We explain it by additional processes like solvation/desolvation or interionic interactions entering into the equilibrium when the adsorbate-adsorbent interaction is relatively weak. The experimental data of the equilibrium surface excess Γ when plotted in the c/Γ *vs* c coordinates yield a set of well fitting straight lines confirming that the adsorption of MV^{2+} follows the Langmuir isotherm. The adsorption parameters obtained from these straight lines are given in Table II. When compared with the 4,4'-bipyridylium dication[17] the Langmuir adsorption coefficient of the MV^{2+} ion for adsorption on Hg is by more than one order of magnitude higher; the reason for this difference can be ascribed to the difference in hydration of the two ions. Greater and stronger hydration of the bipyridylium ion presumably also contributes to the greater surface area occupied at maximum coverage by the ion which by itself is smaller than MV^{2+}. For adsorption of MV^{2+} at a Pt ring-disc electrode at the $E_{1/2}$ potential (−0·69 V) the value for Γ_m was given[29] as 0·20 ± 0·03 nmol cm^{-2} which is within the order of magnitude of our results for Hg; however, the adsorption coefficient of MV^{2+} on Hg comes out almost 100 times higher than the one given for Pt.

According to the data in Table II with increasing negative potential the limiting surface excess Γ_m and the adsorption coefficient β markedly increase. This potential dependence shows two distinctly different regions: at potentials more positive than

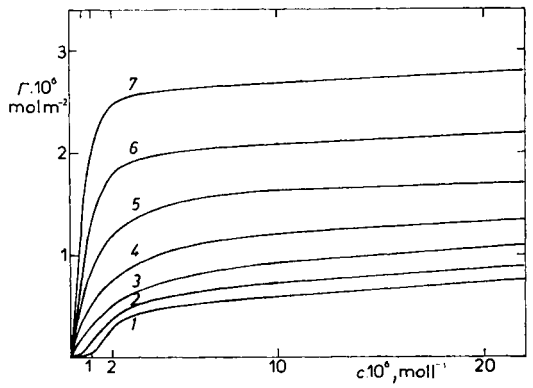

FIG. 4

Adsorption isotherms of $MVCl_2$ up to $2 \cdot 10^{-5}$ mol l^{-1} in 0·1M $NaClO_4$ at potentials: *1* −0·35; *2* −0·40; *3* −0·45; *4* −0·50; *5* −0·55; *6* −0·60; *7* −0·65 V (SCE)

$-0{\cdot}5$ V both Γ_m and β increase aproximately linearly with negative potential, at more negative potentials their steep increase is a function of potential with an exponent higher than 1. At the more positive side the interfacial behaviour of MV^{2+} is obviously similar to that of the bipyridylium dication[15]. The steep increase at the more negative side can be explained by a gradual change of the adsorbed species at the electrode in consequence of a beginning adsorption-coupled electron transfer reaction which makes itself in this way noticeable at $-0{\cdot}5$ V. At potentials more positive all the MV^{2+} ions approaching the electrode from the bulk get reversibly adsorbed with their plane parallel to the surface favouring π-interaction; at potentials more negative some of the MV^{2+} ions approaching the electrode accept an electron at a certain distance from the surface and change into the radical cation $MV^{+\cdot}$ which, polarized in the electric field, gets adsorbed in a position near to perpendicular. The oxidized form, MV^{2+}, is less strongly adsorbed than the reduced form, $MV^{+\cdot}$, and the positive difference between the free energies of adsorption of the reduction product and the reactant shifts the reversible electron transfer to potentials more positive than the standard redox potential of the simple reaction[30].

When an electron transfer reaction initiating mass transfer gets included in electrocapillary measurements, the conditions do not correspond to a pure adsorption equilibrium any more and the Gibbs–Lippmann equation does not hold; however, although not providing exact equilibrium data on such conditions the measurements still supply useful information on adsorption of reaction components and allow conclusions to be drawn on the heterogeneous processes involved in the reaction. In our system, *e.g.*, once the electroreduction starts, the more strongly adsorbable $MV^{+\cdot}$ radical cation begins to replace MV^{2+} from the electrode surface and this change continues throughout the drop life. In the potential range corresponding to

TABLE II

Data of the linearized Langmuir adsorption isotherm obtained from electrocapillary curves measured in solutions of $MVCl_2$ in 0·1M $NaClO_4$

$-E$ V *vs* SCE	Γ_m mol m^{-2}	$1/\Gamma_m$ m^2 mol^{-1}	β m^3 mol^{-1}
0·350	$1{\cdot}07 \cdot 10^{-6}$	$0{\cdot}94 \cdot 10^{6}$	$0{\cdot}98 \cdot 10^{2}$
0·400	$1{\cdot}11 \cdot 10^{-6}$	$0{\cdot}90 \cdot 10^{6}$	$2{\cdot}04 \cdot 10^{2}$
0·450	$1{\cdot}28 \cdot 10^{-6}$	$0{\cdot}78 \cdot 10^{6}$	$3{\cdot}00 \cdot 10^{2}$
0·500	$1{\cdot}36 \cdot 10^{-6}$	$0{\cdot}74 \cdot 10^{6}$	$6{\cdot}12 \cdot 10^{2}$
0·550	$1{\cdot}78 \cdot 10^{-6}$	$0{\cdot}56 \cdot 10^{6}$	$9{\cdot}33 \cdot 10^{2}$
0·600	$2{\cdot}24 \cdot 10^{-6}$	$0{\cdot}45 \cdot 10^{6}$	$16{\cdot}52 \cdot 10^{2}$
0·650	$2{\cdot}82 \cdot 10^{-6}$	$0{\cdot}36 \cdot 10^{6}$	$35{\cdot}50 \cdot 10^{2}$

the limiting current of the first polarographic prewave the whole process goes on only slowly and the results we take from the drop-time measurements are the more remote from the equilibrium data the longer is the drop-time or the more negative is the applied potential. In this respect in Table II only the data measured at potentials less negative than −0·5 V can be regarded as corresponding to true adsorption equilibrium conditions. From the adsorption data we can see how the onset of the electron transfer process brings about the decrease in surface area requirement of the adsorbed species from the maximum, in flat orientation of MV^{2+} with π-interaction, as the proportion of $MV^{+\cdot}$, occupying less area in an inclined orientation, increases.

When followed over a wider concentration range (Fig. 5) the usual shape of isotherms is maintained by the curves at −0·35, −0·40 and −0·45 V. At −0·50 V there appears a small maximum on the curve at concentration of about $5 \cdot 10^{-5}$ mol $\cdot l^{-1}$. With further progress towards negative potential above the concentration $2 \cdot 10^{-5}$ mol l^{-1} the Γ_m values decrease until at $1 \cdot 10^{-4}$ mol l^{-1} they all meet near the value $1{\cdot}2 \cdot 10^{-10}$ mol m^{-2}. This result can be understood when the above mentioned[6,7] reaction of dimerization of the radical cation, $2\,MV^{+\cdot} \rightleftharpoons MV_2^{2+}$, is taken into consideration. At higher concentration of MV^{2+} and at potentials more negative than −0·5 V this reaction competes near the electrode surface with adsorption of the monomer. By stirring during the long drop-time the dimer is brought into the whole volume of the solution and, since it is also adsorbable, it participates with monomer in covering the electrode until, with the given drop-time, at concentration $1 \cdot 10^{-4}$ mol $\cdot l^{-1}$ of MV^{2+} it replaces the monomer completely at the electrode surface. The common value Γ_m for all curves indicates what had been already suggested[31], that in the dimer the aromatic rings of the two moieties are parallel, and that the symmetrical dication dimer MV_2^{2+} gets adsorbed with the rings in parallel with the

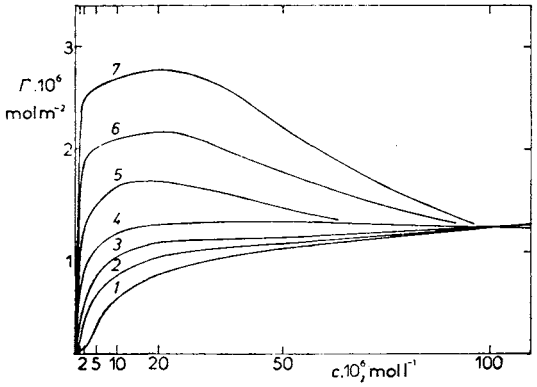

FIG. 5

Adsorption isotherms of $MVCl_2$ up to $1 \cdot 10^{-4}$ mol l^{-1} in 0·1M $NaClO_4$ at potentials: *1* −0·35; *2* −0·40; *3* −0·45; *4* −0·50; *5* −0·55; *6* −0·60; *7* −0·65 V (SCE)

surface occupying very nearly the same area as the primary symmetrical dication MV^{2+}. It was shown elsewhere[32] that in electroreduction of MV^{2+} the dication dimer MV_2^{2+} is formed as a secondary product which undergoes electroreduction in the potential region between the first and second reduction steps of MV^{2+}.

By graphical differentiation of the electrocapillary curves the dependence of the charge density on potential of the electrode has been obtained which is presented in Fig. 6. Unlike in the case of bipyridylium[15] there is no common intercept for the set of curves, as there is no potential of minimum adsorption for MV^{2+}. Here again two potential regions can be distinguished in the dependence: from the beginning of adsorption to about $-0{\cdot}5$ V the negative equilibrium charge density increases steeply with increasing negaiive potential like for bipyridylium; from $-0{\cdot}5$ V where the electroreduction starts participating in the process the increase slows down. Like bipyridylium, the MV^{2+} dication when adsorbed at the electrode in a flat position, attracts electrons from the metal to the surface. From $-0{\cdot}5$ V in the negative direction the charge accumulation at the electrode surface follows the increasing surface concentration of the products of the electrode reaction: the radical cation $MV^{+\cdot}$ at lower volume concentrations of MV^{2+} or at less negative potentials and the growing participation of the dimer MV_2^{2+} in the electrode coverage at higher concentrations or at more negative potentials. In the whole potential range examined the charge density increases with increasing concentration of MV^{2+} along the usual course of an adsorption isotherm to a limit at $5 \cdot 10^{-5}$ mol l^{-1} irrespective of the maxima occurring on the concentration dependence of the surface excess. The accumulation of the negative charge on the electrode surface hence proceeds in a uniform way whether the adsorbed species be MV^{2+}, $MV^{+\cdot}$ or MV_2^{2+}. The last curve in Fig. 6 represents the charge saturation of the mercury surface in contact with MV^{2+} in aqueous solution. The fact that concentrations higher than $5 \cdot 10^{-5}$ mol l^{-1} do not contribute to the equilibrium charge density at the electrode means that at that concentration the surface is completely covered by the adsorbed matter and that only the species coming into closest contact with the metallic surface decide about the charge density on it. The difference in charge density between $5 \cdot 10^{-5}$ mol l^{-1} and $2 \cdot 10^{-4}$ mol l^{-1} solution of MV^{2+} at the positive side of the electrocapillary curve is probably due to a particular structure of the surface layer of the associations between MV^{2+} and anions, evident also on the Γ–E curves.

From the curves in Figs 3 and 6 the dependence of the charge density, q, on the surface excess, Γ, can be found; this is given in Fig. 7. For the potentials $-0{\cdot}35$, $-0{\cdot}40$ and $-0{\cdot}45$ V the dependence has the same characteristic course as in the case of the bipyridylium dication. From $-0{\cdot}5$ V to more negative potentials the sequence of the initial linear parts acquires an opposite direction of the slopes. This is due to the gradual change of the initial composition of the surface layer with increasing proportion of $MV^{+\cdot}$ to MV^{2+}. The steep increase of negative charge density after the initial moderate increase is an obvious consequence of the increase

of the average Γ_m value due to continued replacement of the MV^{2+} ions by the $MV^{+\cdot}$ radical ions in the adsorbed layer as the faradayic current continues flowing throughout the whole drop-life.

Polarographic Measurements

The First Prewave

From the data for Γ_m in Table II it follows that in the potential region positive of $-0{\cdot}50$ V the cation MV^{2+} is adsorbed with its plane flat on the electrode surface. On the d.c. polarographic curves recorded with high sensitivity the adsorption of MV^{2+} is indicated by a small cathodic current which extends towards positive potentials as the adsorption extends (Fig. 8). As shown in Fig. 8, this small cathodic current precedes the first prewave with half-wave potential at $-0{\cdot}5$ V and, like the limitng current of this prewave, increases with concentration of MV^{2+} to a limit reached at about $5 \cdot 10^{-5}$ mol l^{-1}. A similar cathodic current had been found[33] to precede the adsorption prewave of methylene blue. It is obviously due to the nega-

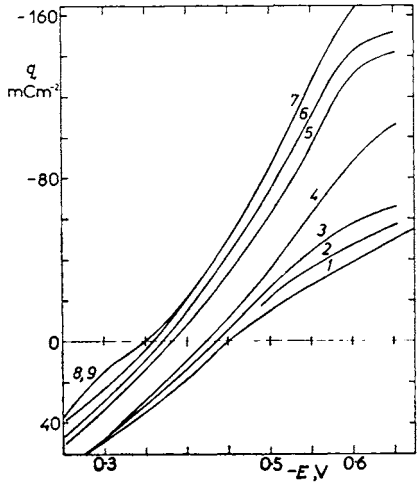

FIG. 6

Dependence of the equilibrium density q on potential obtained from the curves in Fig. 2 (corresponding curves numbering)

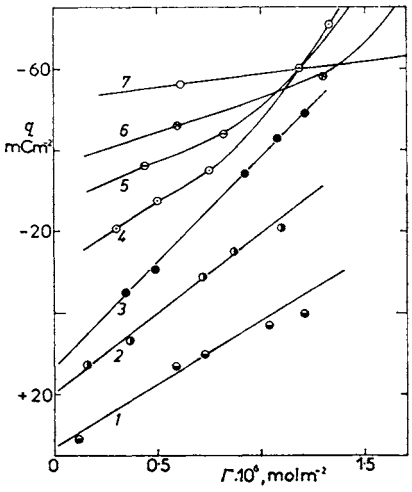

FIG. 7

Dependence of the equilibrium charge density q on the surface excess Γ for potentials: *1* $-0{\cdot}35$; *2* $-0{\cdot}40$; *3* $-0{\cdot}45$; *4* $-0{\cdot}50$; *5* $-0{\cdot}55$; *6* $-0{\cdot}60$; *7* $-0{\cdot}65$ V (SCE), obtained from the data in Figs 3 and 6

tive charge attracted to the electrode surface by the positively charged planar aromatic species in π-interaction with the metal. The essential difference between the charge density–potential curves in Fig. 6 and the polarographic charging current accompanying adsorption shown in Fig. 8 is in the degree of attainment of adsorption equilibrium: while the data from electrocapillary measurements up to the potential of $-0{\cdot}5$ V refer to equilibrium attained with a long drop-time and stirring, the polarographic adsorption current at low concentrations of MV^{2+} corresponds to a non-equilibrium state; at higher concentrations when the diffusion is able to supply sufficient amount of MV^{2+} for equilibrium to be reached within the usual short drop-time of 3 – 5 s, the equilibrium surface concentration is already near the complete coverage.

The first polarographic prewave appears in the potential region where, measured at equilibrium conditions, an adsorption interaction of MV^{2+} with the electrode surface takes place and, besides, a transport-controlled faradayic process begins to make itself noticeable. However, within the short drop-time in polarography this faradayic process comes into force only at more negative potentials and hence the wave observed on polarographic curves is connected only with the adsorption interaction of MV^{2+} with the electrode surface. The main characteristics of the prewave as well as the electrocapillary equilibrium data up to its half-wave potential are analogous to that of the bipyridylium ion[15]. We suggest that like there it is due to the surface redox process of the cations adsorbed with the heterocyclic rings in parallel with the electrode surface:

$$MV^{2+} \rightleftharpoons (MV^{2+})_\pi$$

$$(MV^{2+})_\pi + e \rightleftharpoons (MV^{+\cdot})_\pi ,$$

where the subscript π denotes the π-interaction in adsorbed state.

During the time of contact with the electrode the system of π electrons of the adsorbed MV^{2+} cation, which acts as electron acceptor due to the effect of the two positive charges, is in the field of a higher negative charge density than the

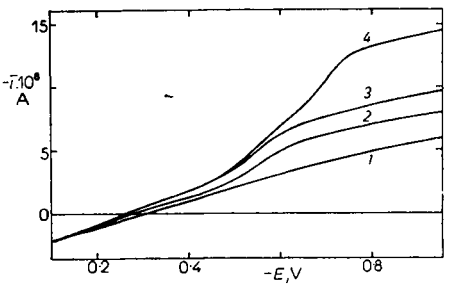

FIG. 8

D.c. polarographic curves of 0·1M $NaClO_4$ solution containing: *1* 0; *2* 4; *3* 5; *4* 7 . 10^{-5} mol l^{-1} $MCVl_2$

system of a cation in the solution. (In an analogous case, in viologen-capped porphyrins, where π-interaction exists between MV^{2+} and the prophyrins, a polarization of electron density from porphyrin to viologen has been observed[34].) In reduction of MV^{2+} the newly accepted electron joins the delocalized system of π electrons of the radical cation $MV^{+\cdot}$; the electroreduction of the adsorbed MV^{2+} cation then takes place in a less negative range of externally applied potential than the reduction of the non-adsorbed cation and on the polarization curves it appears as an adsorption pre-wave or pre-peak[35]. In the reversible adsorption equilibrium at the potential of the limiting current of the first prewave each elementary act of adsorption is accompanied by reduction of the MV^{2+} ion and each desorption by its reoxidation so that the composition of the solution near the electrode surface remains unchanged. The surface redox process hence cannot be observed in potentiometry or in potentiostatic electrolysis with stationary electrodes[35]. It shows the behaviour characteristic of charging or adsorption currents: in d.c. polarography the limiting height of the surface redox wave is directly proportional to the pressure of mercury above the tip of the capillary which is directly proportional to the rate of change of the electrode surface dA/dt; at a slow rate of drop growth the surface redox prewave becomes indistinguishable by the side of the main wave (Fig. 9). Similarly, if recorded with the "tast" or "current sampling" polarographic techniques when the current is measured towards the end of a longer drop-time when dA/dt is small, the polarographic curve does not show the surface redox wave. On voltammetric curves the cathodic and anodic peaks due to the surface redox process appear on the positive side of the main redox peaks providing the rate of change of potential, dE/dt, is sufficiently high (Fig. 10). At low scanning rates the surface redox peaks on the

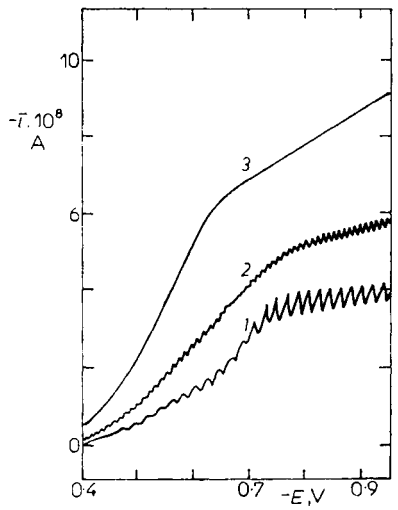

FIG. 9

Effect of the mercury pressure upon the separation of the first prewave and the main wave on d.c. polarographic curves of $5 . 10^{-5}$ mol l^{-1} $MVCl_2$ in 0·1M $NaClO_4$. The drop-time measured at −0·8 V was: *1* 5·6; *2* 3·0; *3* 1·5 s.

voltammetric curves ultimately merge with the charging current (*cf.* results in[36]). In phase-selective a.c. polarography the surface redox process of MV^{2+} is characterized by a peak on both, the in-phase and out-of-phase, components of the cell impedance which remains prominent up to high frequencies[10,25].

When the electrode gets covered by a surfactant more strongly adsorbed than MV^{2+}, the first prewave due to the surface redox process is eliminated and the reduction of MV^{2+} takes place in the normal, main wave with its half-wave corresponding to the potentiometric redox potential, as is demonstrated in Fig. 11. (The same effect as shown in the figure was achieved by a 10^{-4} mol l^{-1} solution of tetrabutylammonium perchlorate; *cf.* also results in[36].)

The Second Prewave

While the first prewave pertains to a redox process in itself, *i.e.*, to the surface redox process, the short characteristics of the second prewave given in the introduction and displayed in Fig. 1 indicate a direct connection of this prewave with the redox process in the main wave. The second prewave begins to appear on polarographic curves only at MV^{2+} concentration of about $1{\cdot}5 \cdot 10^{-4}$ mol l^{-1} with the usual drop-times of 3–5 seconds, and from that concentration it accompanies the main wave. With the foot of the main wave it shifts to positive potentials when the MV^{2+}

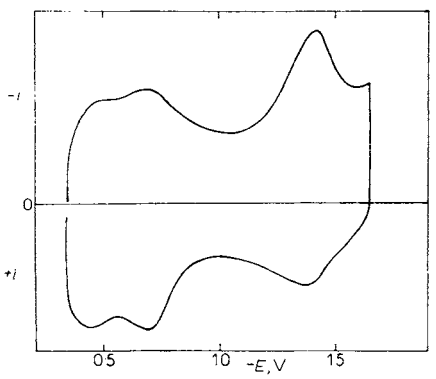

FIG. 10

Cyclic voltammetric curve of $1 \cdot 10^{-5}$ mol . l^{-1} $MVCl_2$ in 0·1M $NaClO_4$ obtained with a hanging mercury drop electrode at scanning rate of 0·32 V s^{-1} showing a pair of reversible prepeaks due to the surface redox and two pairs of reversible peaks due to two primarily reversible processes of the two-stage reduction of MV^{2+}

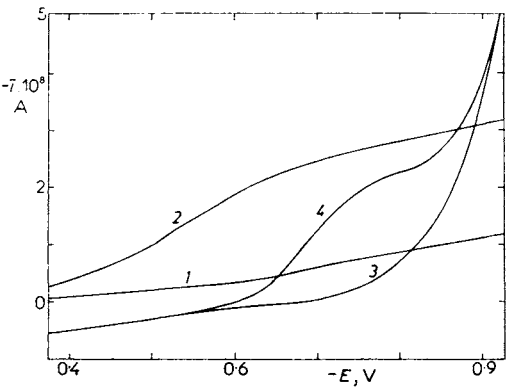

FIG. 11

Effect of surfactant upon the surface redox reaction. D.c. polarographic curves of: *1* 0·1M $NaClO_4$; *2* $+4 \cdot 10^{-5}$ mol l^{-1} $MVCl_2$; *3* 0·1M $NaClO_4$ + $1 \cdot 10^{-4}$ mol l^{-1} erythrosin; *4* $+4 \cdot 10^{-5}$ mol l^{-1} $MVCl_2$

concentration increases. At higher temperatures, while the first prewave only slightly shifts to negative potentials, the second prewave disappears entirely from the polarographic curve. It does not occur with solutions containing either adsorbable substances like alcohols or buffer components at higher concentrations, or anionic substances at low concentrations, like in pure water or in buffers at low degree of dissociation. A marked feature of this prewave, in contrast to the drawn-out first prewave, is the steep increasing part becoming more prominent at higher concentrations, suggesting that the current determining reaction is a fast process. This conclusion follows also from a study of *i–t* curves or from slow-scan voltammetric experiments with slowly growing or stationary mercury drop electrodes. On *i–t* curves in the potential region around −0·60 V there appears at a certain moment a sudden sharp and narrow cathodic peak (Fig. 12); the time of appearance of this discontinuous increase of current is gradually delayed when the potential is made more negative. When the *i–t* curves were followed with a solution which after long experimenting contained some form of reduction products of MV^{2+}, the peak was appearing on the *i–t* curves irreproducibly, at random times. The peak occurs over a potential span of about 60 mV; at the side of negative potentials the shape of the *i–t* curves changes in a way indicating a complex adsorption process accompanying the faradayic reaction. An analogous peak on slow scan voltammograms has an anodic counterpart on the reverse branch of the curve which proves reversibility of the process. The potential difference between the cathodic and anodic peaks is less than 30 mV; its value depends on the scan rate and on composition of the solution.

The experimental facts lead to the conclusion that the second prewave is due to reduction of MV^{2+} followed by formation over the electrode of a primarily two-

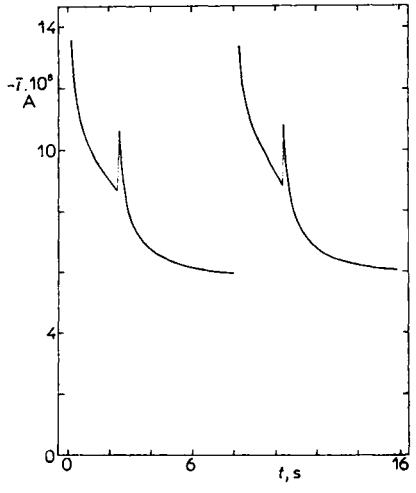

FIG. 12

Instantaneous current–time curves at constant potential of −0·625 V with $2 . 10^{-4}$ mol $. l^{-1}$ $MVCl_2$ in 0·1M $NaClO_4$

-dimensional crystalline layer of a sparingly soluble salt of the radical cation $MV^{+\cdot}$ with an anion from the solution – a similar case as was described in electroreduction of 4,4'-bipyridyl[15]. Like there, the difference in potentials of the main wave and the second prewave is due to the free energy of crystallization and adsorption of the salt; for MV^{2+} this is obviously less than the energy for the corresponding salt of 4,4'--bipyridyl which gives as a rule a more prominent reduction prewave. On top of the two-dimensional layer of the adsorbed oriented salt the growth of the crystal can continue in the third dimension from the side of the solution when further radical cations are generated by electron transfer through the primary layer. In d.c. polarography the limiting current of the second prewave increases linearly with increasing negative potential; the inverse slope of this linear dependence is an indication of the resistance of the crystalline layer: with longer drop-time the layer on the surface of the drop grows thicker, its resistance accordingly increases and the slope of the limiting current is smaller. The formation of the crystalline layer can take place only when special conditions are fulfilled: there must be sufficiently high concentration both of MV^{2+} and of the anion in the space close to the electrode surface and the electrode potential must be sufficiently negative so that the reduction of MV^{2+} followed by adsorption of the radical $MV^{+\cdot}$ takes place at an appropriate rate and a nucleus for the crystallization can be formed, but not too negative, as the higher rate of generation of the radical cation leads to formation of the adsorptive dimer MV_2^{2+}. The region of potentials over which the salt of the radical cation is formed at the electrode is limited at the negative side on the polarization curves by an abrupt increase of current which obviously denotes the change of reaction mechanism due to the replacement of the layer of salt from the electrode surface by the adsorption of the dimer. The dimerization of the radical cation is obviously one of the factors noxious to crystallization of the radical cation salt layers in the technique of the display systems (see, *e.g.*,[37] and papers cited therein). The steep slope of the ascending part of the second prewave is due to the fast growth of the layer following the nucleation process. In the old solution some dispersed particles of reduction products when coming at random into contact with the surface can presumably initiate the nucleation – hence the random occurrence of the current peaks observed on the *i–t* curves.

The Main Wave

In Fig. 11 it can be seen that when an interaction between MV^{2+} and $MV^{+\cdot}$ and the electrode is prevented by blocking the electrode surface, the electroreduction of MV^{2+} takes place already at the lowest concentrations in the potential range of the main wave with the half-wave potential at $-0{\cdot}69$ V. The electron transfer in the main wave hence corresponds to the simple redox reaction without either MV^{2+} or $MV^{+\cdot}$ interacting with the electrode. In absence of surfactants the electrode gets

covered by a layer of the radical cation, its salt or its dimer, as was shown above, in the potential region positive of the main wave. The electron transfer in the main wave, therefore, proceeds at the electrode as in a homogeneous redox process, unhindered by the surface coverage.

At concentration $5 \cdot 10^{-4}$ mol l^{-1} of MV^{2+} the top of the front part of the polarographic wave is distorted with a tendency for a maximum to occur – the maxima do actually occur at still higher concentrations[36,38]. This is presumably due to fast dimerization of the radical cation in solution near the electrode and to replacement of the monomer by the dimer at the electrode surface which produces fast changes of surface tension in course of drop life. Such conditions could account also for the region of irreproducible drop-times at the electrocapillary curve shown in Fig. 1.

CONCLUSIONS

The study of the one-electron reduction of the MV^{2+} cation at mercury electrodes by means of polarographic techniques and electrocapillary measurements has confirmed that the basically simple reaction is in practice a complex process due to homogeneous and heterogeneous interactions of the components of the redox system, MV^{2+}, $MV^{+\cdot}$ and MV_2^{2+}, with solution components and the electrode surface. The stages involved in the reduction, in the sequence proceeding towards negative potentials, are the following:

1. at positively charged electrode, $E > E_{p.z.c.}$, reversible adsorption of MV^{2+} with its plane in parallel with the electrode surface enabling π-interaction with the metal

$$MV^{2+} \rightleftharpoons (MV^{2+})_\pi ;$$

2. at negatively charged electrode, $-0{\cdot}5 < E < E_{p.z.c.}$, surface electron transfer in π-interaction with the electrode (surface redox process), 1. polarographic prewave

$$(MV^{2+})_\pi + e \rightleftharpoons (MV^{+\cdot})_\pi$$

3. at $E \leqq -0{\cdot}5$ V, with long drop-times and lower concentrations observed already at $E = -0{\cdot}5$ V, in polarography at $E < -0{\cdot}5$ V, electron transfer followed by reversible adsorption of $MV^{+\cdot}$ in a position inclined towards surface

$$MV^{2+} + e \rightleftharpoons MV^{+\cdot} \qquad (a)$$

$$MV^{+\cdot} \rightleftharpoons (MV^{+\cdot})_{ads} \qquad (b)$$

4. at $E \leqq -0{\cdot}5$ V; with long drop-times and higher concentrations observed already at $E = -0{\cdot}5$ V, in polarography at $E < -0{\cdot}5$ V, formation and reversible adsorp-

tion of the radical dimer MV_2^{2+} in π-interaction with the electrode; occurs after stage (*3a*) and competes with (*3b*)

$$2\,MV^{+\cdot} \rightleftharpoons MV_2^{2+}$$

$$MV_2^{2+} \rightleftharpoons (MV_2^{2+})_\pi$$

5. at $-0{\cdot}69\ V < E < -0{\cdot}5\ V$, occurs with sufficiently high concentration of MV^{2+} and of anion X^-, electron transfer followed by surface crystallization of a sparingly soluble salt of radical cation; takes place after stage *3.* and is hindered by stage *4.*, 2. polarographic prewave

$$(MV^{+\cdot})_{ads} + X^- \rightleftharpoons [MV^{+\cdot}X^-]_{ads.\,cryst.}$$

6. at $E \leqq -0{\cdot}69$ V, electron transfer through a surface layer of electrolytic products adsorbed at the electrode surface, polarographic main wave

$$MV^{2+} + e \rightleftharpoons MV^{+\cdot}\,.$$

REFERENCES

1. Michaelis L.: Biochem. Z. *250*, 564 (1932).
2. Mulazzani Q. G., Venturi M., Hoffman M. Z.: J. Phys. Chem. *89*, 722 (1985).
3. Okura I., Kaji N., Aono S., Kita T., Yamada A.: Inorg. Chem. *24*, 451 (1985).
4. Ebbesen T. W., Manring L. E., Peters K. S.: J. Am. Chem. Soc. *106*, 7400 (1984).
5. Michaelis L., Hill E. S.: J. Gen. Physiol. *16*, 859 (1933).
6. Schwarz W. M. jr: *Thesis*. Univ. of Wisconsin, 1961; Diss. Abstr. *22*, 1843 (1961).
7. Kosower E. M., Cotter J. L.: J. Am. Chem. Soc. *86*, 5524 (1964).
8. Neta P., Richoux M.-C., Harriman A.: J. Chem. Soc., Faraday Trans. 2, *81*, 1427 (1985).
9. Steckhan E., Kuwana T.: Ber. Bunsenges. *78*, 253 (1974).
10. Pospíšil L., Kůta J., Volke J.: J. Electroanal. Chem. *58*, 217 (1975).
11. Regis A., Corset J.: J. Chim. Phys. *78*, 687 (1981).
12. Furlong D. N., Tricot Y. M., Swift J. D., Sasse W. H. F.: Aust. J. Chem. *37*, 703 (1984).
13. Ebbesen T. W.: J. Phys. Chem. *88*, 4131 (1984).
14. Enea O.: Electrochim. Acta *30*, 13 (1985).
15. Heyrovský M., Novotný L.: This Journal *52*, 54 (1987).
16. Novotný L., Smoler I.: J. Electroanal. Chem. *146*, 183 (1983).
17. Novotný L., Smoler I., Kůta J.: This Journal *48*, 964 (1983).
18. Müller O. H.: Ann. N. Y. Acad. Sci. *40*, 91 (1940).
19. Elofson R. M., Edsberg R. L.: Can. J. Chem. *35*, 646 (1957).
20. Volke J.: Chem. Listy *61*, 429 (1967).
21. Volke J.: This Journal *33*, 3044 (1968).
22. Osa T., Kuwana T.: J. Electroanal. Chem. *22*, 389 (1969).
23. Ito M., Kuwana T.: J. Electroanal. Chem. *32*, 415 (1971).
24. Homer R. F., Mees G. C., Tomlinson T. E.: J. Sci. Food Agric. *11*, 309 (1960).
25. Pospíšil L.: unpublished results.
26. Pospíšil L., Kůta J.: J. Electroanal. Chem. *90*, 231 (1978).

27. Ebbesen T. W., Ferraudi G.: J. Phys. Chem. *87*, 3717 (1983).
28. Novotný L., Kalvoda R.: This Journal *51*, 1595 (1986).
29. Albery W. J., Bartlett P. N.: J. Electroanal. Chem. *182*, 7 (1985).
30. Brdička R.: Z. Elektrochem. *48*, 278 (1942).
31. Evans A. G., Evans J. C., Baker M. W.: J. Chem. Soc., Perkin Trans. 2, *1977*, 1787.
32. Heyrovský M.: J. Chem. Soc., Chem. Commun. in press.
33. Heyrovský M.: unpublished results.
34. Leighton P., Sanders J. K. M.: J. Chem. Soc., Chem. Commun. *1984*, 856.
35. Heyrovský M., Vavřička S., Heyrovská R.: J. Electroanal. Chem. *46*, 391 (1973).
36. Kobayashi K., Niki K.: Chem. Lett. *1982*, 829.
37. Bewick A., Lowe A. C., Wederell C. W.: Electrochim. Acta *28*, 1899 (1983).
38. Black C. C. jr: Biochim. Biophys. Acta *120*, 332 (1966).